

Chaotic Motion Around Stellar Objects with Octupolar Deformation: Newtonian and Post Newtonian Approaches

Javier Ramos-Caro,^{*} Framsol López-Suspes,[†] and Guillermo A. González[‡]
*Grupo de Investigación en Relatividad y Gravitación, Escuela de Física,
Universidad Industrial de Santander, A.A. 678, Bucaramanga, Colombia*

Regular and chaotic test particle motion in gravitational fields due to stellar bodies with quadrupolar and octupolar deformation are studied using Poincaré surfaces of section. In first instance, we analyze the purely Newtonian case and we find that the octupolar term induces a distortion in the KAM curves corresponding to regular trajectories as well as an increase in chaoticity, even in the case corresponding to oblate deformation. Then we examine the effect of the first general relativistic corrections, provided by the post Newtonian approach. For typical values of the post Newtonian multipoles we find that the phase-space structure practically remains the same as in the classical case, whereas that for certain larger values of these multipoles the chaoticity vanishes. This important fact provides an interesting example of a situation where a non-integrable dynamical system becomes integrable through the introduction of a large perturbation.

PACS numbers: 95.10.Fh, 05.45.-a, 04.25.Nx

I. INTRODUCTION

As is suggested by a wide variety of observational evidences, many astrophysical objects can be modeled as axially symmetric bodies with prolate or oblate deformation. For example, it is known that the Earth has non vanishing quadrupolar and octupolar moments, as a consequence of its oblate shape[1]. Also, many galaxies with a large disc component can be assumed as axisymmetric oblate bodies with a large quadrupolar moment and, in some cases, with a comparable octupolar deformation due to the remaining components (for example, the halo). Likewise, there are galaxy clusters with a cigarlike shape[2] and many dwarf galaxies that can be considered as nearly axisymmetric prolate deformed objects[3]. Although in the above cases the quadrupolar moment it is considered to be the major deviation from the spherical symmetry, there are situations (for example, some metallic clusters) where the octupolar deformation play a significant role[4, 5].

The motion of test particles around such stellar objects is a problem of wide physical interest. The case of attraction centers described by monopolar plus quadrupolar terms has been extensively studied by Guerón and Letelier, from a classical and relativistic standpoint, showing that the inclusion of external multipolar moments can induce chaos[6, 7, 11]. In Newtonian gravity, as well as in general relativity, chaos can be found when the source has prolate deformation and the chaoticity grows by increasing the quadrupolar moment. On the other hand, it seems to be that the case corresponding to oblate deformation does not lead to chaotic motion, indeed for a very large quadrupolar deformation. However, inclusion of octupolar deformation can also induce chaos, as it was shown by Heiss, Nasmitdinov and Radu[10] and Li[14] in the case of an harmonic oscillator.

In the present paper we investigate the motion of test particles in axially symmetric gravitational potentials that are the sum of a monopole, a quadrupole and an octupolar term (only external multipole moments will be considered). At the first instance, in Sec. II, we shall perform the analysis in the context of Newtonian gravity by examining how the structure of the Poincaré surfaces of section is determined by the octupolar moment. We find that, even in the case of oblate deformation, modest values of the octupolar moment induce chaotic motion. Then, in order to compare how these results are modified by considering the first general relativistic corrections, we shall introduce in Sec. III the post Newtonian (1PN) approach, where the gravity is described by the classical Newtonian potential and another additional field, which is written in terms of the 1PN multipolar moments. Contrary to the usual statement that integrable problems in Newtonian theory become non integrable in general relativity, we find that, for certain values of the 1PN multipolar moments, the test particle motion is regular in situations where the Newtonian theory predicts chaos.

^{*}e-mail: javiramos1976@gmail.com

[†]e-mail: framsol@gmail.com

[‡]e-mail: gonzalez@gag-girg-uis-net

II. TRANSITION RING-SPINDLE TORUS AND CHAOS INDUCED BY OCTUPOLAR DEFORMATION

Consider a test particle moving in the axially symmetric gravitational field generated by a stellar body with quadrupolar and octupolar deformation. In cylindrical coordinates (R, z, φ) , its potential has the form

$$\Phi = -\frac{\alpha}{\sqrt{R^2 + z^2}} - \frac{\beta(2z^2 - R^2)}{2(R^2 + z^2)^{5/2}} - \frac{\gamma(2z^3 - 3zR^2)}{2(R^2 + z^2)^{7/2}}. \quad (1)$$

Since we are interested on to describe the exterior test particle motion, we consider only external multipolar moments. In the above equation α is the monopole term that equals to Gm , where m is the total mass of the source and G is the gravitational constant. The quadrupolar term, denoted by β , usually represents the major deviation from spherical symmetry. In particular, if $\beta > 0$ the source has prolate deformation and if $\beta < 0$ we have the case corresponding to oblate deformation. The octupolar moment γ describes the asymmetry of the source with respect to the equatorial plane, i.e. its ‘‘shape-of-pear’’ deformation. Both β and γ are related to the source’s density $\rho(R, z)$ through the equations [9]

$$\beta = 2\pi \int_0^\infty r'^4 dr' \int_0^\pi d\theta' \sin \theta' P_2(\cos \theta') \rho(r', \theta'), \quad (2)$$

$$\gamma = 2\pi \int_0^\infty r'^5 dr' \int_0^\pi d\theta' \sin \theta' P_3(\cos \theta') \rho(r', \theta'), \quad (3)$$

where we have used spherical coordinates $r = \sqrt{R^2 + z^2}$, $\cos \theta = z/\sqrt{R^2 + z^2}$ and P_l denotes the Legendre polynomial of order l .

The motion of a test particle in a gravitational field described by (1), obeys the relations

$$\dot{R} = V_R, \quad (4)$$

$$\dot{z} = V_z, \quad (5)$$

$$\dot{V}_R = -\frac{\partial \Phi_{ef}}{\partial R}, \quad (6)$$

$$\dot{V}_z = -\frac{\partial \Phi_{ef}}{\partial z}, \quad (7)$$

where Φ_{ef} is the effective potential, given by

$$\Phi_{ef} = \Phi + \frac{\ell^2}{2R^2}. \quad (8)$$

Here, $\ell = R^2 \dot{\varphi}$ is the axial specific angular momentum that is conserved as a consequence of the axial symmetry. The second integral of motion is the total specific energy, given by

$$E = (V_R^2 + V_z^2)/2 + \Phi_{ef}. \quad (9)$$

According to eqs. (4)-(9), the motion is restricted to a three dimensional phase space (R, z, V_R) . This fact enable us to introduce the Poincaré surfaces of section method, in order to investigate the trajectories of test particles.

In Fig. 1 we plot a typical $z = 0$ surface of section corresponding to test particle motion in the presence of a gravitational field due to a prolate deformed source whom octupolar moment vanishes (from here on, we choose $\alpha = 1$, without loss of generality). We note a central and lateral regular regions composed by ring torus (ring KAM curves). They are enclosed by a chaotic region containing two small resonant islands near its top and bottom edges. In Fig. 2 we switch on the octupolar moment ($\gamma = 0.02$), maintaining the same prolate deformation. The resulting surface of section presents a more prominent chaotic region, since in this case the outer zones of resonant islands have overlapped. The regular regions now contains ‘‘spindle’’ torus. They can be viewed clearly in the central region and scarcely insinuated in the lateral zone. In Fig. 3, as a consequence of increase the octupolar moment to $\gamma = 0.04$, the chaotic region is more prominent (the lateral regular zone has disappeared), as well as the central spindle KAM curves. Finally, Figs. 4 and 5 show the effect caused by the progressive rise in the octupolar deformation, starting from a regular prolate situation.

The fact that by switching on the octupolar moment increases the chaoticity and leads to apparition of spindle torus, can be viewed even in the case corresponding to oblate deformation, which commonly presents regular motion

(in fact, there is a wide numerical evidence that particles moving around a monopole plus an oblate quadrupole are not chaotic). Fig. 6 shows the transition from regularity to chaos by increasing γ . With $E = -0.32$, $\ell = 1.1$ and $\beta = -0.2$, we start from $\gamma = 0$ (Fig. 6a) which corresponds to a regular motion. The case $\gamma = 0.02$ is also regular but the KAM curves has been distorted to spindles. In Fig. 6c ($\gamma = 0.04$) the distortion is more prominent and finally, when γ has increased up to 0.06 we note the apparition of a chaotic region enclosing the spindles.

III. NEWTONIAN VS POST-NEWTONIAN MULTIPOLAR MOMENTS

The post newtonian approximation (commonly called as 1PN approach) gives the first general relativistic corrections (up to order v^2/c^2 , where c is the speed of light) to the motion equations, when we deal with particles moving non relativistically ($v \ll c$) in the presence of strong gravitational fields. We are interested in the situation when a test particle moves around a static axially symmetric source. As it was shown by Rezanian and Sobouti [13], in the stationary case we have an integral of motion $E = v^2/2 + \Phi + (2\Phi^2 + \Psi)/c^2$ that can be considered as a generalization of the classical specific energy. Here, Φ and Ψ obeys the Poisson equations

$$\nabla^2 \Phi = \frac{4\pi G}{c^2} T^{00}, \quad (10)$$

$$\nabla^2 \Psi = 4\pi G [T^{00} + T^{ii}], \quad (11)$$

where T^{00} and T^{ii} denotes the 0-th and 2-th terms in v/c in the 00-components of the energy momentum tensor. T^{ii} represents the trace of T^{ij} up to order 2 in v/c . Relations (10) and (11) suggest that both Φ and Ψ can be expanded in external multipolar fields. In particular, since T^{00} represents the source's density [12, 13], the expansion for Φ is the same as in equation (1).

In the case of Ψ , we can write

$$\Psi = -\frac{\tilde{\alpha}}{\sqrt{R^2 + z^2}} - \frac{\tilde{\beta}(2z^2 - R^2)}{2(R^2 + z^2)^{5/2}} - \frac{\tilde{\gamma}(2z^3 - 3zR^2)}{2(R^2 + z^2)^{7/2}}, \quad (12)$$

where $\tilde{\alpha}$, $\tilde{\beta}$, and $\tilde{\gamma}$ play the role of the post Newtonian monopole, quadrupole and octupole moments, respectively. In a similar way as in (2)-(3), they are given by

$$\tilde{\alpha} = 2\pi \int_0^\infty r'^2 dr' \int_{-1}^1 dx' [T^{00} + T^{ii}], \quad (13)$$

$$\tilde{\beta} = 2\pi \int_0^\infty r'^4 dr' \int_{-1}^1 dx' P_2(x') [T^{00} + T^{ii}], \quad (14)$$

$$\tilde{\gamma} = 2\pi \int_0^\infty r'^5 dr' \int_{-1}^1 dx' P_3(x') [T^{00} + T^{ii}], \quad (15)$$

where $x' = \cos \theta' = z'/\sqrt{R'^2 + z'^2}$.

The motion equations for a test particle can be derived from the Hamiltonian

$$H = \frac{1}{2} (V_R^2 + V_z^2) + \frac{\ell^2}{2R^2} + \Phi + \frac{1}{c^2} (2\Phi^2 + \Psi), \quad (16)$$

(note that $\ell = R^2 \dot{\varphi}$ is an integral of motion) and can be written as

$$\dot{V}_R = -\frac{\partial U_{ef}}{\partial R}, \quad (17)$$

$$\dot{V}_z = -\frac{\partial U_{ef}}{\partial z}, \quad (18)$$

where we have defined the post Newtonian effective potential U_{ef} as

$$U_{ef} = \Phi + \frac{1}{c^2} (2\Phi^2 + \Psi) + \frac{\ell^2}{2R^2}. \quad (19)$$

From eqs. (17), (18) and (19), along with (1) and (12), we can study the trajectories of test particles in a similar way than in the Newtonian case, as was performed in section II.

For example, Fig. 8 show a $z = 0$ surface of section corresponding to $\ell = 0.9$, $E = -0.4$, $\alpha = 1$, $\beta = 0.3$, $\gamma = 0.02$ (the same parameters as in Fig. 3), $\tilde{\alpha} = 10^5$, $\tilde{\beta} = -2 \times 10^4$ and $\tilde{\gamma} = 10^4$ (according with the system of units employed, we have to take $c = 10^4$). It has similar features as in Fig. 3, but in this case there is not lateral resonant islands. If one increase adequately the post Newtonian quadrupole and octupole, an interesting fact occurs: the chaotic zones disappear and the resulting surface of section reveals completely regular motion. Indeed, as it is shown in Fig. 9, the regular regions are made by rings instead of spindle torus, for these particular values of multipole parameters. In Figure 7 we show the contours of the effective potential corresponding to these two cases. The former exhibits $z = 0$ asymmetry while the second is practically symmetric with respect to the equatorial plane.

IV. CONCLUDING REMARKS

Octupolar deformation in astrophysical objects can introduce significant modifications to the phase-space structure corresponding to test particles moving around prolate or oblate centers of attraction. Apart from an increasing in the chaoticity, the apparition of spindle torus in regular regions is a remarkable effect caused by the asymmetry of the source with respect to its equatorial plane. A larger equatorial asymmetry involves more distorted spindle KAM curves and more prominent stochastic regions in the phase-space. This fact carries dramatic consequences in the case of oblate deformed sources, which usually are associated with regular motion. Here, chaos emerges once we switch on the octupole moment.

When the first general relativistic corrections are taken into account, through the post Newtonian approach, the structure in the phase space remains practically the same as in Newtonian gravity, for typical values of 1PN multipolar moments. However, there are certain large values for which the test particle motion becomes regular. This fact introduces an interesting example where a non-integrable dynamical system becomes integrable through the introduction of a large perturbation.

Acknowledgments

J. R-C. and F. L-S want to thank the financial support from *Vicerrectoría Académica*, Universidad Industrial de Santander.

-
- [1] D. Boccaletti and G. Pucacco. *Theory of Orbits, Volume 1*. Springer. Third edition (2004).
 - [2] A. R. Cooray. Mon. Not. R. Astron. Soc. 313, 783 (2000).
 - [3] B. S. Ryden. Astrophys. J. 461, 146 (1996).
 - [4] I. Hamamoto, B. Mottelson, H. Xie and X. Z. Zhang. Z. Phys. D 21, 163 (1991).
 - [5] S. Frauendorf and V. V. Pashkevich. Z. Phys D 26, S98 (1993). Z. Phys. D 21, 163 (1991).
 - [6] E. Guéron and P. Letelier. Phys. Rev. E 66, 04661 (2002).
 - [7] E. Guéron and P. Letelier. Phys. Rev. D 56, Brief Rep. 12 (1997).
 - [8] G. Benettin, L. Galgani, and J. M. Strelcyn. Phys. Rev. A, 14(6), 2338 (1976).
 - [9] J. Binney and S. Tremaine *Galactic Dynamics*. Princeton University Press (1987).
 - [10] W. D. Heiss, R. G. Nasmitdinov and S. Radu. Phys. Rev. Lett., 72 (15), 2351 (1994).
 - [11] E. Guéron and P. Letelier. Phys. Rev. E, 63, 035201 (2001).
 - [12] S. Weinberg. *Gravitation and Cosmology*. John Wiley (1972).
 - [13] V. Rezanía and Y. Sobouti. Astron. Astrophys. 354, 1110 (2000)
 - [14] Jun-Qing Li. J. Phys. G: Nucl. Part. Phys. 24, 1021 (1998).

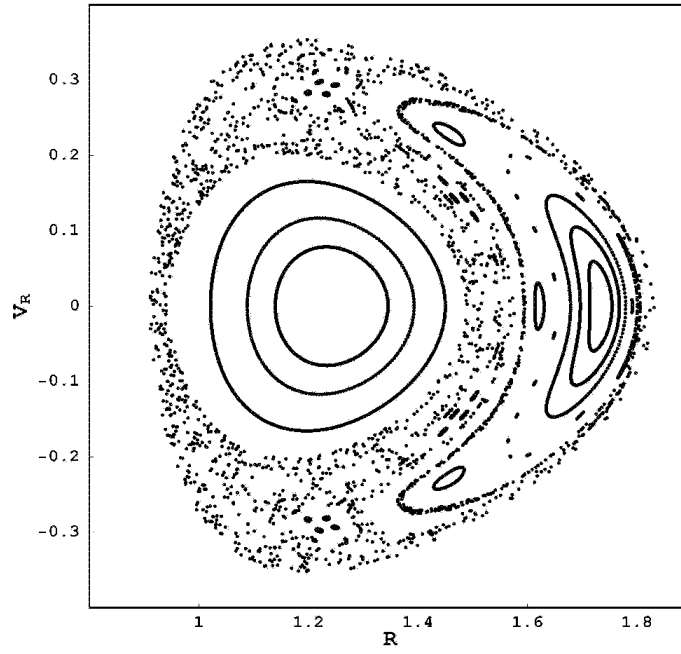


FIG. 1: Surface of section for some orbits with $\ell = 0.9$, $E = -0.4$, in a potential characterized by $\alpha = 1$, $\beta = 0.3$ and $\gamma = 0$.

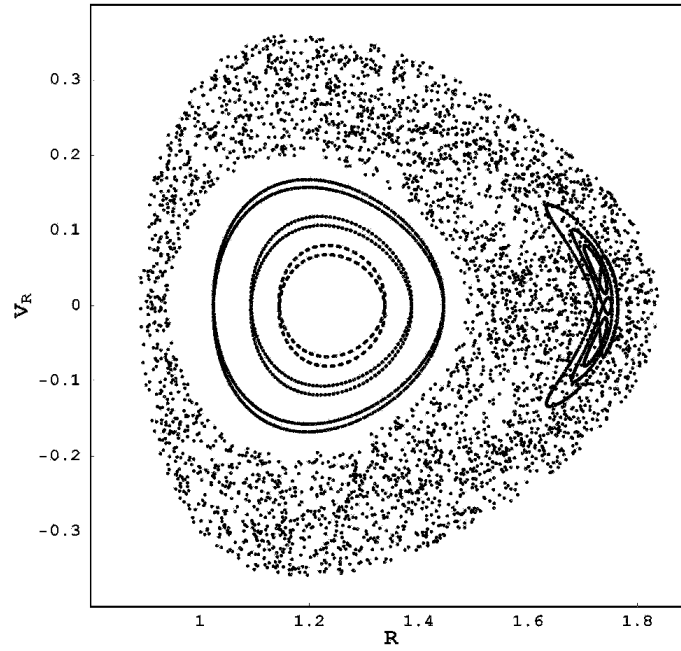


FIG. 2: Surface of section for the same initial conditions of the previous figure. We maintain the values $\ell = 0.9$, $E = -0.4$, $\alpha = 1$ and $\beta = 0.3$, but now $\gamma = 0.02$.

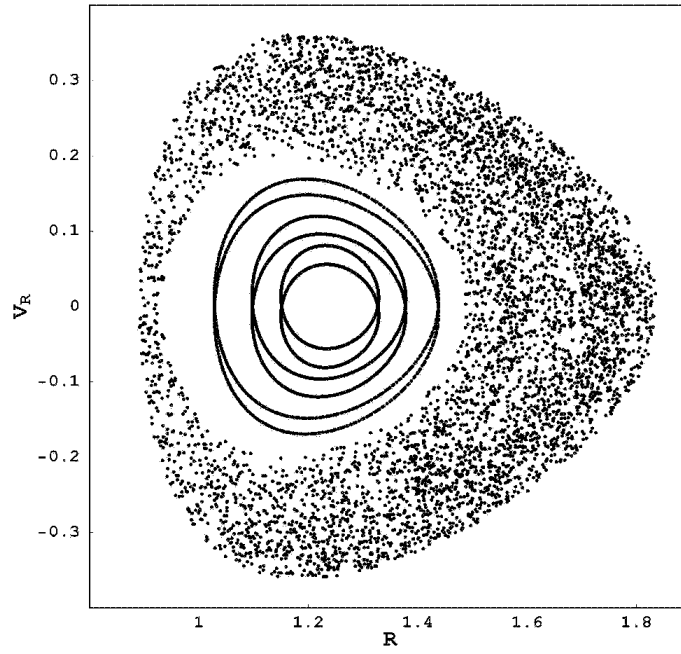


FIG. 3: In this case, setting the same values of the two previous figures but $\gamma = 0.04$, we have a prominent chaotic zone enclosing three "spindle" KAM curves.

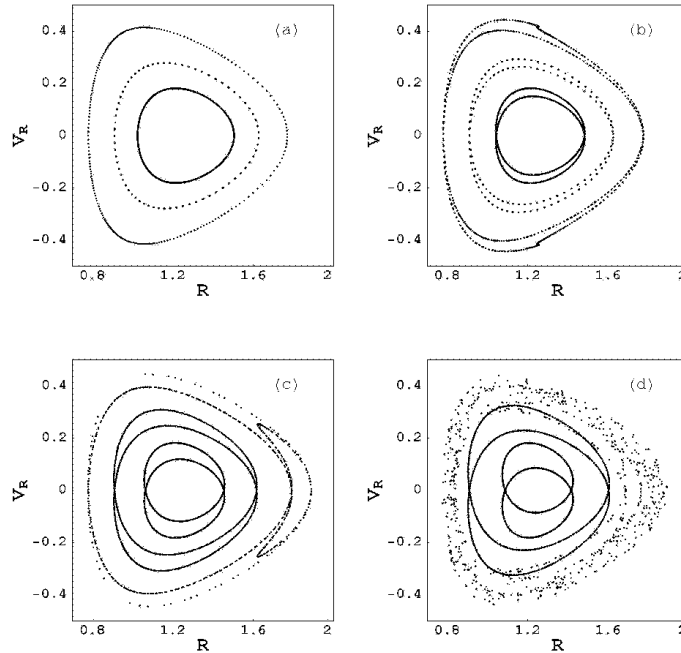


FIG. 4: Surfaces of section for $\ell = 0.9$, $E = -0.4$, $\alpha = 1$, $\beta = 0.2$ and (a) $\gamma = 0$; (b) $\gamma = 0.02$; (c) $\gamma = 0.04$; (d) $\gamma = 0.06$. In each case, they are generated by three orbits with initial conditions (i) $z = 0$, $R = 0.91$, $V_R = 0$; (ii) $z = 0$, $R = 0.78$, $V_R = 0$ and (iii) $z = 0$, $R = 1.16$, $V_R = 0.18$.

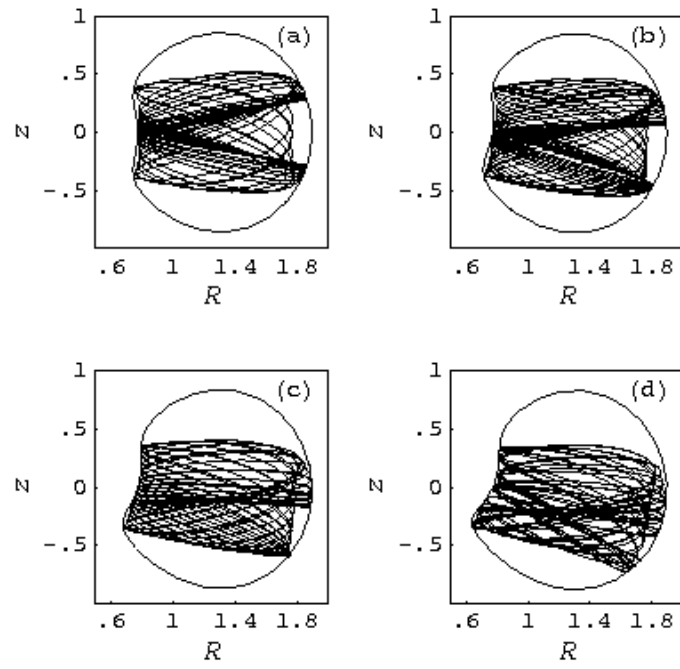


FIG. 5: An orbit in the meridional plane with initial conditions $z = 0$, $R = 0.78$, $V_R = 0$ and the same parameters considered above. Again we have the cases (a) $\gamma = 0$; (b) $\gamma = 0.02$; (c) $\gamma = 0.04$; (d) $\gamma = 0.06$

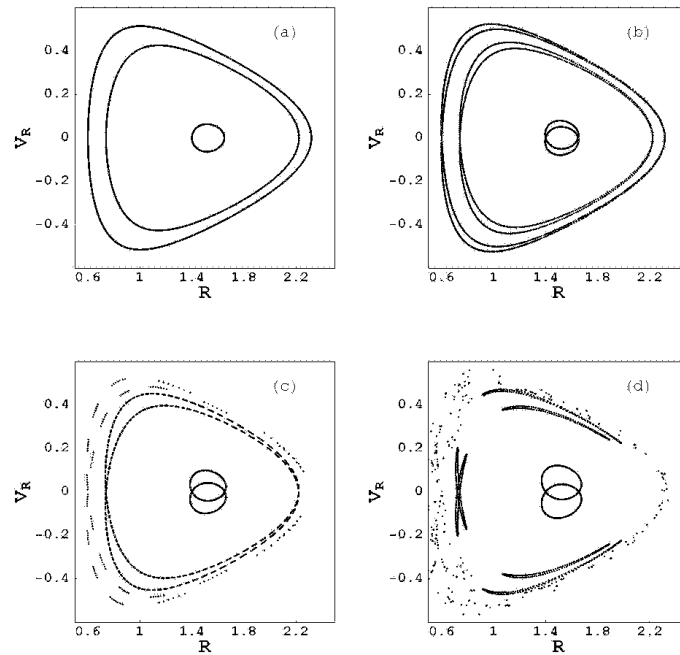


FIG. 6: Surfaces of section for $\ell = 1.1$, $E = -0.32$, $\alpha = 1$, $\beta = -0.2$ and (a) $\gamma = 0$; (b) $\gamma = 0.02$; (c) $\gamma = 0.04$; (d) $\gamma = 0.06$. In each case, they are generated by three orbits with initial conditions (i) $z = 0$, $R = 0.91$, $V_R = 0$; (ii) $z = 0$, $R = 0.78$, $V_R = 0$ and (iii) $z = 0$, $R = 1.16$, $V_R = 0.18$.

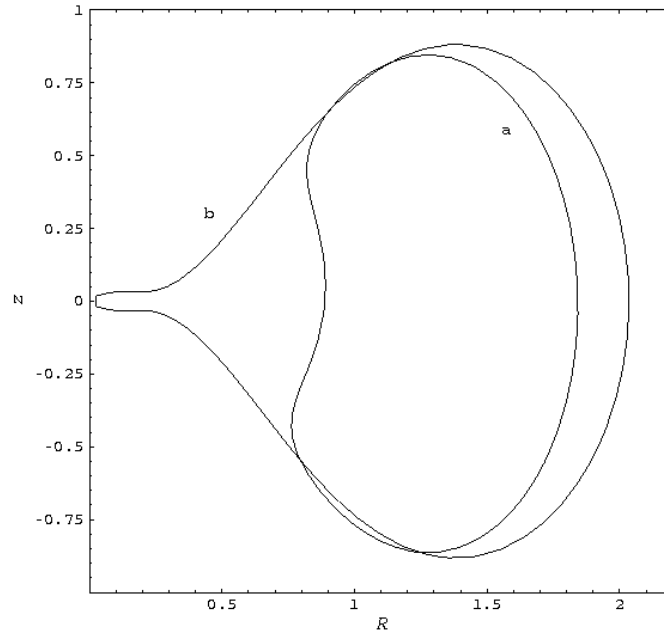


FIG. 7: Contours of the effective potential U_{ef} , for $\alpha = 1$, $\beta = 0.3$, $\gamma = 0.02$, $\tilde{\alpha} = 10^5$ and (a) $\tilde{\beta} = -2 \times 10^4$, $\tilde{\gamma} = 10^4$; (b) $\tilde{\beta} = -4 \times 10^7$ and $\tilde{\gamma} = -2 \times 10^6$

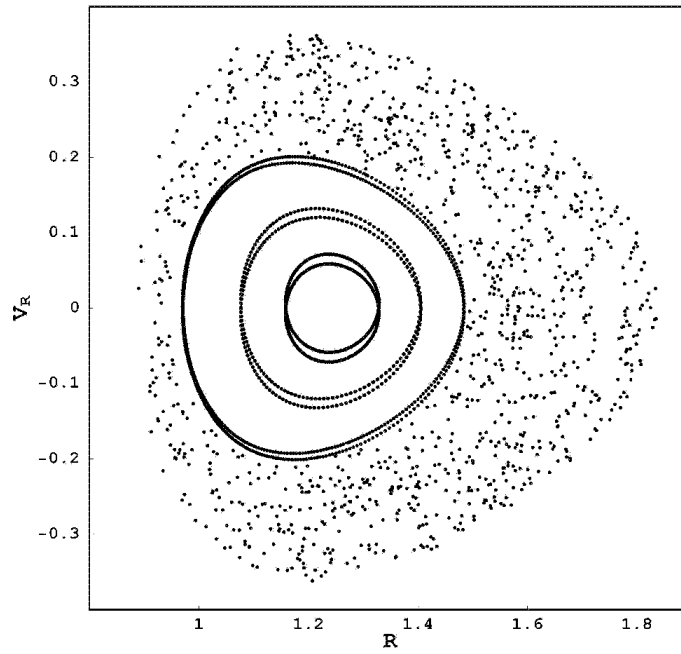


FIG. 8: In this case, we have chosen the same parameters as in Fig. 3 along with $\tilde{\alpha} = 10^5$, $\tilde{\beta} = -2 \times 10^4$, $\tilde{\gamma} = 10^4$.

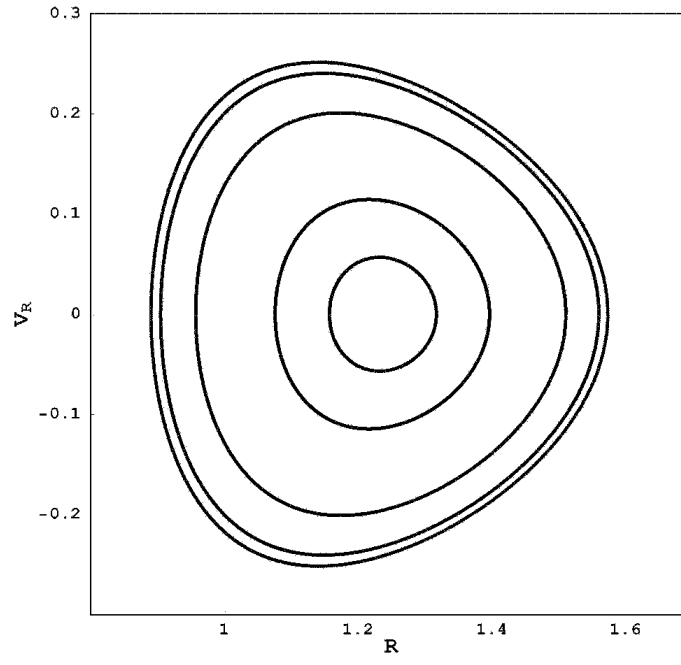


FIG. 9: Now we keep the same values of E , ℓ , α , β , γ , $\tilde{\alpha}$ as well as the same initial conditions as in previous figure, but $\tilde{\beta} = -4 \times 10^7$ and $\tilde{\gamma} = -2 \times 10^6$. With these values of post Newtonian multipolar moments we have a surface of section corresponding to regular motion